MARS^2: Agile and Robust Flight Control of Modular Aerial Robot Systems

Rui Huang, Zhiqian Cai, Siyu Tang, Jialin Zhang, Zhenyu Zhang, Lin Zhao

***Abstract*— Modular Aerial Robot Systems (MARS), composed of multiple self-reconfigurable drone units, offer high adaptability to diverse mission scenarios and fault conditions. Existing docking mechanism designs for MARS are prone to significant oscillations during docking and separation. Moreover, their control systems are conservative and sensitive to disturbances, which only allow quasi-static hovering flight and waypoint-based flight. To address these disadvantages, we first develop a highly integrated mechanical system that significantly simplifies passive docking, detection-free passive locking, and active separation by using a single servo motor. Our experimental results demonstrate substantial improvements in smooth and stable docking and separation performance. To fully unleash the redundant control actuation of MARS, we further propose an equivalent modeling framework that abstracts arbitrary MARS configurations into a unified virtual quadrotor representation. Building on this abstraction, we design and implement a model predictive control algorithm for MARS of arbitrary configurations. Moreover, we develop efficient algorithms to map the virtual thrust and torque control commands to those of individual units. To the best of our knowledge, this work presents the first real-world demonstrations of agile trajectory tracking and obstacle avoidance with active yaw angle control for MARS. The videos and source code of this work are available at `https://nus-core.github.io/assets/standalone/MARS2/index.html`.**

I. Introduction

Inspired by collective behavior in nature, researchers have proposed modular aerial robot systems (MARS) capable of in-flight reconfiguration. By allowing multiple units to physically assemble in mid-air, these systems can adaptively increase their payload capacity based on the object's weight and adjust their morphology to accommodate irregular shapes. Existing work has focused on mid-air aerial docking [1], in-flight separation [2], and self-reconfiguration algorithms [3]. To further enable agile flight in MARS, we present a novel integrated docking mechanism and an equivalent modeling framework. Specifically, our main contributions are as follows:

1) To achieve high-reliability docking and separation, we propose a novel mechanical design that integrates passive docking, detection-free passive locking, and active separation for MARS.
2) We propose a novel equivalent modeling framework that transforms diverse modular configurations into a single virtual quadrotor. This abstraction allows direct application of existing control methods originally designed for single quadrotor. To validate its effectiveness, we implement an model predictive control (MPC), which can be generalized to other model-based frameworks.
3) We further validate the proposed equivalent model and control strategy through real-world experiments. Our goal is to demonstrate that MARS can unlock the full range of capabilities typically reserved for traditional quadrotors.

Rui Huang, Siyu Tang, Jialin Zhang, Zhenyu Zhang, and Lin Zhao are with the Department of Electrical and Computer Engineering, National University of Singapore, Singapore 117583, Singapore (email: ruihuang@u.nus.edu, e1352616@u.nus.edu, e1538883@u.nus.edu, zhenyuzhang@u.nus.edu, elezhli@nus.edu.sg). Zhiqian Cai is with the Engineering Design and Innovation Centre, National University of Singapore, Singapore 117583, Singapore (email: zhiqian@u.nus.edu)

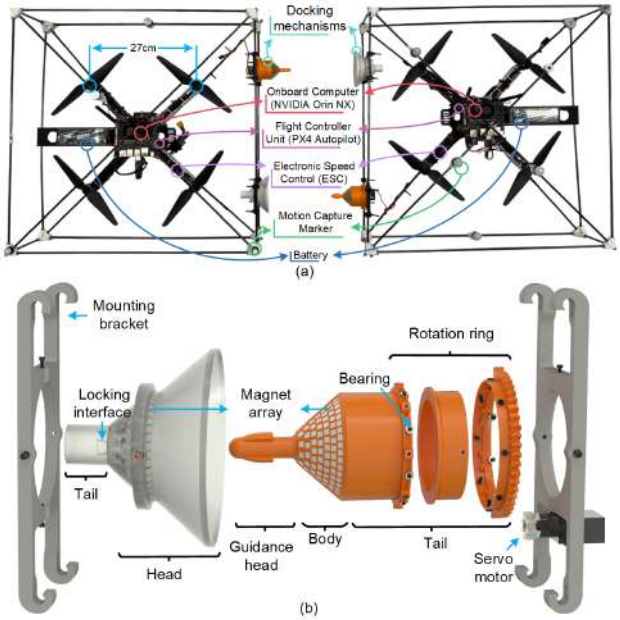

Fig. 1. System architecture specifications. (a) Flight platform hardware components, with male and female docking mechanisms mounted on one side of the drone. (b) The female docking component includes a docking head with an embedded magnet array, a tail with a locking interface, and a mounting bracket. The male docking component includes a guidance head with two convex locking structures, a male body, a tail directly connected to a rotation ring, and a servo motor mounted on the bracket.

II. System Design and Modeling

A. MARS Design

The mechanical design integrates passive docking, detection-free passive locking, and active separation for MARS, as shown in Fig. 1. The key features of our mechanism are as follows:

1) Integrated docking-locking-separation mechanism: Unlike prior works that rely solely on permanent magnets for either docking or separation [1], [2], [4], our design

unifies all three functionalities within a simple and compact structure.

2) Detection-free passive mechanical locking: Upon successful docking, the mechanism passively locks without requiring additional sensors or detection logic. This contrasts with [5], which necessitates real-time docking verification to avoid actuator interference or failure.

3) Actively actuated, repulsion-assisted separation: The entire transition between docking, locking, and separation modes is actuated using a single micro-servo motor, in contrast to the dual-servo, multi-link actuation system used in [5], offering a more simplified implementation. Specifically for detachment, unlike [2], our method leverages magnetic repulsion to achieve separation, enhancing both safety and robustness without requiring large sliding angles.

4) Robustness of docking and separation: Owing to the designed docking guidance head for the male connector, our mechanism achieves higher docking tolerance than those reported in [1], [4], [5]. Moreover, aerial experiments validate the robustness of our system. Compared to [1], [4], our design shows markedly reduced altitude oscillation during docking, and compared to [2], it enables faster separation with lower attitude disturbances.

B. Equivalent Model Predictive Control

The equivalent model transforms diverse modular configurations into a unified control abstraction, and abstracts MARS as a virtual quadrotor that produces equivalent total forces and torques to those of the original MARS. The objective is to simplify the control strategy for implementation, enabling the direct application of existing control methods developed for single quadrotor. Figure 3 shows the virtual quadrotors based on different configurations, where the standard $\times$-shaped virtual quadrotor leverages the orientation of MARS and maximizes the net torque, while the flexible model generates arbitrary shaped virtual quadrotor.

To compute the control commands for each unit effectively, we then implement an MPC framework that bridges the virtual quadrotor model and the modular hardware system. As illustrated in Fig. 2, the controller first solves an MPC optimization problem based on the dynamics and constraints of the virtual quadrotor. The resulting control inputs are then mapped to the individual modular units by assuming that the control inputs of virtual and actual quadrotors produce the same collective force and torque.

III. Real-world Experiments

A. Mid-air docking

Figure 4(a) illustrates the complete process of mid-air docking. Initially, the hovering drone remains stationary at a fixed position. Once the docking unit reaches the designated target location, it takes off, tracks the hovering unit (red arrow), and prepares to execute the docking operation at 00:47:00, successfully establishing a connection at 00:47:19.

Figure 4(c) presents the time-series acceleration, attitude, and position data for both drones during the docking maneuver. During docking, the z-axis acceleration of the hovering

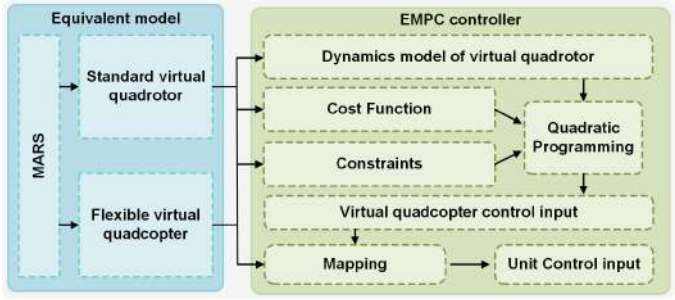

Fig. 2. Equivalent model predictive control framework for MARS. To obtain the control inputs of the virtual quadrotor, we solve a quadratic programming problem that minimizes the cost function. The resulting virtual control inputs are mapped to the actual unit control inputs.

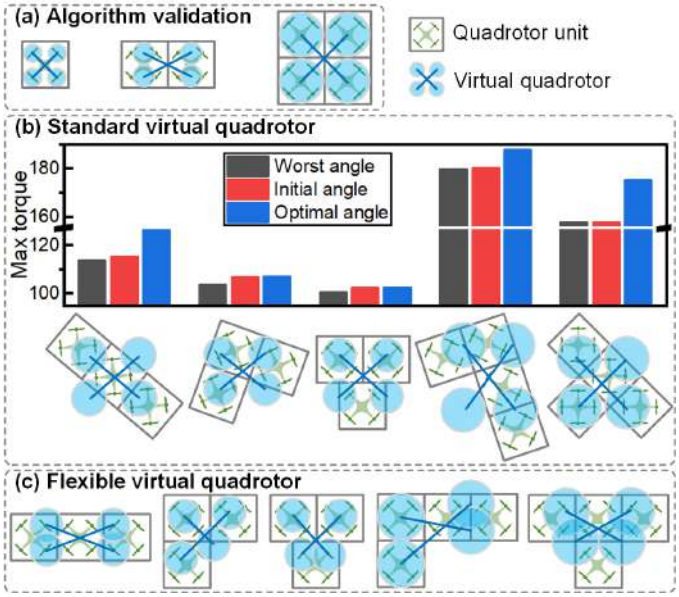

Fig. 3. Equivalent model for MARS. (a) Algorithm validation using virtual quadrotors formed by 1, 2, and 4 units in MARS. (b) Performance evaluation on standard virtual quadrotors, showing up to 11.13% improvement (average 5.03%) over baseline configurations with initial angle 0°. (c) Equivalent models for flexible virtual quadrotors, illustrating the computation of virtual representations for various modular assemblies.

unit briefly peaks at 12.63 m/s^2 due to the collision and stabilizes within 1 s. Similar transient variations are observed along the x- and y-axes, with maximum accelerations reaching 3.47 m/s^2 for both drones. **These results demonstrate that our design enables smooth docking with minimal attitude disturbance, confirming the feasibility of the docking mechanism and the effectiveness of the proposed docking control system.**

B. Active repulsion-based separation

We design the separation mode for the docking mechanism by only adding a mini servo motor (20 g) to rotate the male docking mechanism from the lock mode to the separation mode. Fig. 5(a) presents the aerial separation experiment. The top panel shows a composite image: two drones remain docked in midair. Upon reaching the target location, the male docking mechanism switches from lock mode to separation mode at 00:13:14, activating a repulsive force that facilitates detachment (red arrow). Subsequently, at

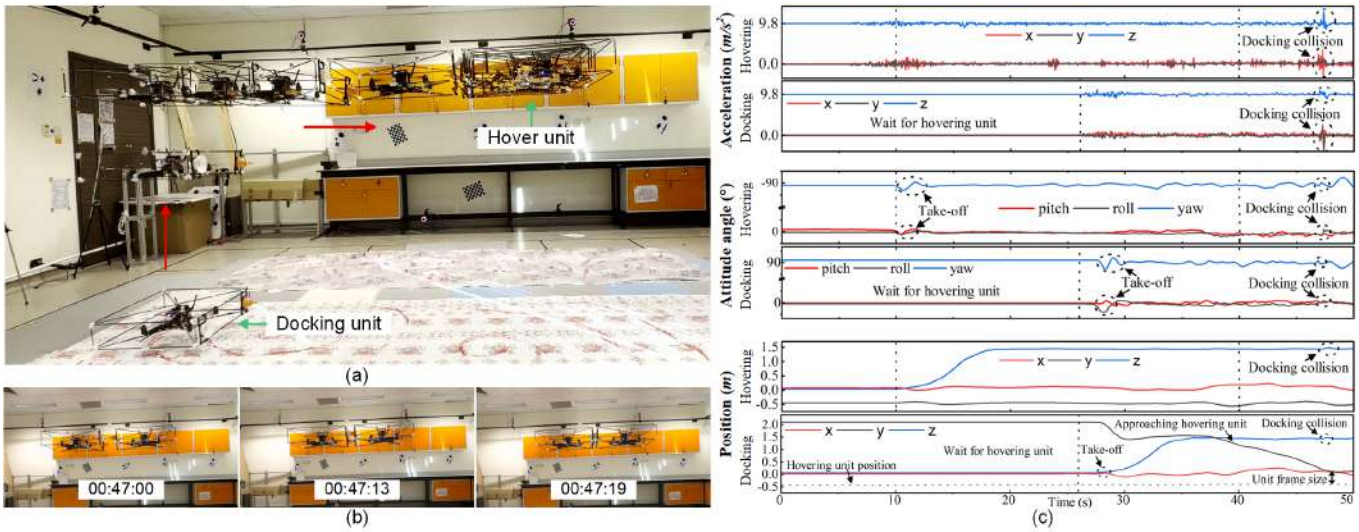

Fig. 4. Mid-air docking demonstration. The timer is formatted as *minute:second:millisecond*. (a) The hover unit maintains a stable position while the docking unit takes off, approaches, and actively adjusts its trajectory to achieve precise mid-air docking. (b) The docking process starts at 00:47:00 and successfully ends at 00:47:19. (c) Time-series plots of acceleration, attitude angles, and position for both units, showing active trajectory correction of the docking unit, and the docking collision, illustrating the effectiveness of the proposed mid-air docking approach.

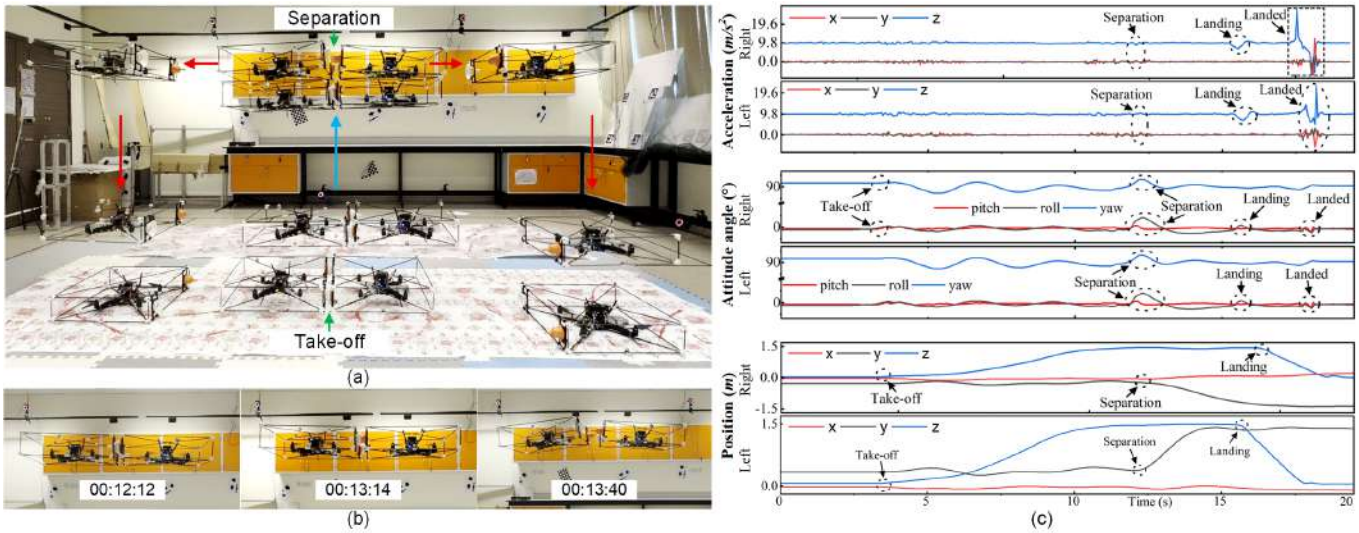

Fig. 5. Mid-air separation demonstration. The timer is formatted as *minute:second:millisecond*. (a) Two drones docked together take off simultaneously , perform a mid-air separation maneuver, and then independently land. (b) After switching to separation mode, the drones successfully disengage from each other during the time interval 00:12:12 to 00:13:40. (c) Experimental data during the demonstration, showing the acceleration along x, y, z axes, attitude angles (pitch, roll, yaw), and position trajectories. The key events is marked on the plot, including take-off, mid-air separation, and landing states. The drones exhibit only slight variations in attitude during the separation, highlighting the dynamic response and stability of the system.

00:13:40, position control drives the two drones to separate. The bottom sequence captures these key timestamps, where the male component detaches from the female component under the assistance of the repulsion force.

Figure 5(c) plots the position, attitude, and acceleration profiles during the maneuver. The roll angle remains within $\pm 5^\circ$ throughout separation, indicating minimal attitude disturbance and validating the stability of our active separation design. The slight roll variations stem primarily from position control rather than any destabilizing force. Additionally, the acceleration remains near zero, and the position trajectories are smooth and continuous. In contrast, although prior work [2] did not provide numerical separation curves, their videos exhibit significant attitude oscillations and positional disturbances during separation.

C. Trajectory tracking

1) Circular trajectory tracking: Fig. 6(a) illustrates the circular trajectory tracking performance of MARS. A composite image captures the full execution of a 0.6 m-radius circular path, demonstrating stable and continuous flight. The results confirm that the proposed control method achieves accurate position and attitude tracking throughout the maneuver. **This demonstrates MARS's ability to perform trajectory tracking with minimal position error, highlighting the feasibility and effectiveness of the equivalent model and MPC controller.**

2) Agile trajectory tracking: To further evaluate the agile flight capability of the MARS, we set the desired velocity to exceed 2 m/s. As shown in Fig. 6(b), the MARS successfully tracks the circular trajectory while maintaining roll and pitch

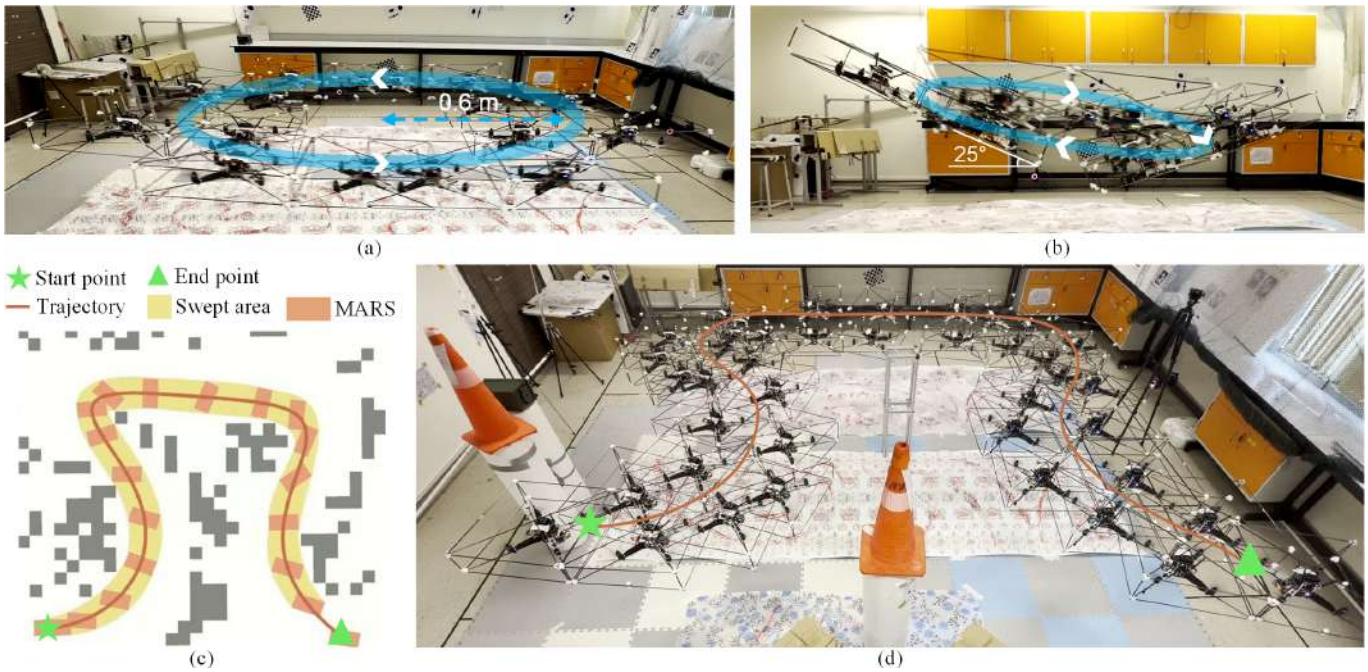

Fig. 6. Trajectory tracking experiments. (a) Composite image showing the trajectory tracking process with velocity of 1 m/s. (b) Agile trajectory tracking performance. The MARS maintains speeds above 2 m/s while following a circular trajectory of 0.5 m radius. The roll and pitch angles reach approximately 25°, demonstrating agile maneuverability. (c) Collision-free trajectory generation. (d) Real-world experiments demonstrate the robust tracking performance of obstacle avoidance.

angles of approximately 25°. It is worth noting that our MARS system is significantly larger than typical agile aerial robots, commonly sized at 160×160 mm or 100×100 mm, whereas our platform measures 1200×570 mm. This scale imposes additional challenges for agile maneuvering. The results demonstrate that our MPC not only enables accurate trajectory tracking but also ensures robust performance under high-speed, agile flight conditions, outperforming prior works [1], [4].

3) Collision-free trajectory tracking: In this subsection, we demonstrate that the MPC-based MARS can accurately follow ideal collision-free trajectories generated by [6], as shown in Fig.6(c). Real-world experiments were conducted to track this trajectory. As shown in Fig.6(d), yaw-angle tracking is more challenging for MARS because its moment of inertia about the z-axis is larger than that of a single unit. Nevertheless, our MPC successfully follows the reference trajectory without collisions. **These results highlight that the proposed MPC can serve as a general controller for MARS, enabling trajectory planning in the same manner as traditional aerial robots, using only the geometric shape and equivalent model of the MARS.**

IV. Conclusion

We addressed two core challenges for MARS: (1) stable aerial docking and separation, and (2) agile trajectory tracking with obstacle avoidance. An integrated docking-locking-separation mechanism was experimentally validated for robustness and reliability, while a novel equivalent modeling framework abstracted multi-unit MARS as a single virtual quadrotor, enabling direct use of general model-based controllers. Our system achieved reduced oscillations and enabled first real-world agile flight demonstrations, including agile trajectory tracking and obstacle avoidance.

References

[1] D. Saldana, B. Gabrich, G. Li, M. Yim, and V. Kumar, "Modquad: The flying modular structure that self-assembles in midair," in *2018 IEEE International Conference on Robotics and Automation (ICRA)*. IEEE, 2018, pp. 691–698.

[2] D. Saldana, P. M. Gupta, and V. Kumar, "Design and control of aerial modules for inflight self-disassembly," *IEEE Robotics and Automation Letters*, vol. 4, no. 4, pp. 3410–3417, 2019.

[3] R. Huang, S. Tang, Z. Cai, and L. Zhao, "Robust self-reconfiguration for fault-tolerant control of modular aerial robot systems," in *2025 International conference on robotics and automation (ICRA)*. IEEE, 2025. [Online]. Available: https://arxiv.org/abs/2503.09376

[4] G. Li, B. Gabrich, D. Saldana, J. Das, V. Kumar, and M. Yim, "Modquad-vi: A vision-based self-assembling modular quadrotor," in *2019 International Conference on Robotics and Automation (ICRA)*. IEEE, 2019, pp. 346–352.

[5] J. Sugihara, M. Zhao, T. Nishio, K. Okada, and M. Inaba, "Beatle—self-reconfigurable aerial robot: Design, control and experimental validation," *IEEE/ASME Transactions on Mechatronics*, 2024.

[6] R. Huang, Z. Zhang, S. Tang, Z. Cai, and L. Zhao, "Robust fault-tolerant control and agile trajectory planning for modular aerial robotic systems," in *2025 IEEE/RSJ international conference on intelligent robots and systems (IROS)*. IEEE, 2025. [Online]. Available: https://arxiv.org/abs/2503.09376